PB1-F2, an Influenza A Virus-Encoded Proapoptotic Mitochondrial Protein, Creates Variably Sized Pores in Planar Lipid Membranes

A. N. Chanturiya,[1] G. Basañez,[2] U. Schubert,[3,4] P. Henklein,[5] J. W. Yewdell,[6] and J. Zimmerberg[1]*

Laboratory of Cellular and Molecular Biophysics, National Institute of Child Health and Human Development,[1] and Laboratory of Viral Diseases, National Institute of Allergy and Infectious Diseases,[6] National Institutes of Health, Bethesda, Maryland 20892; Heinrich-Pette-Institute of Experimental Virology and Immunology, University of Hamburg, Hamburg,[3] Institute of Clinical and Molecular Virology, University of Erlangen-Nürnberg, Erlangen,[4] and Institute of Biochemistry, Humboldt University, Berlin,[5] Germany; and Unidad de Biofisica (Centro Mixto UPV/EHU-CSIC), Universidad del Pais Vasco (UPV/EHU), 48080 Bilbao, Spain[2]

A frameshifted region of the influenza A virus PB1 gene encodes a novel protein, termed PB1-F2, a mitochondrial protein that can induce cell death. Many proapoptotic proteins are believed to act at the mitochondrial outer membrane to form an apoptotic pore with lipids. We studied the interaction of isolated, synthetic PB1-F2 (sPB1-F2) peptide with planar phospholipid bilayer membranes. The presence of nanomolar concentrations of peptide in the bathing solution induced a transmembrane conductance that increased in a potential-dependent manner. Positive potential on the side of protein addition resulted in a severalfold increase in the rate of change of membrane conductance. sPB1-F2-treated membranes became permeable to monovalent cations, chloride, and to a lesser extent, divalent ions. Despite various experimental conditions, we did not detect the distinctive conductance levels typical of large, stable pores, protein channels, or even pores that are partially proteinaceous. Rather, membrane conductance induced by sPB1-F2 fluctuated and visited almost all conductance values. sPB1-F2 also dramatically decreased bilayer stability in an electric field, consistent with a decrease in the line tension of a lipidic pore. Since similar membrane-destabilizing profiles are seen with proapoptotic proteins (e.g., Bax) and the cytoplasmic helix of human immunodeficiency virus gp41, we suggest that the basis for sPB1-F2-induced cell death may be the permeabilization and destabilization of mitochondrial membranes, leading to macromolecular leakage and apoptosis.

A novel influenza A virus (IAV) protein, PB1-F2, was recently described (12, 17). This 87-amino-acid, 11-kDa protein is encoded by an alternative reading frame in the PB1 gene, probably through a ribosomal scanning mechanism. PB1-F2 has several unusual features compared with other influenza virus gene products, including variable expression in individual infected cells and mitochondrial localization. PB1-F2 expression is associated with accelerated IAV-induced apoptosis of infected monocytes. Exposure of cells to the synthetic version of PB1-F2 also induces apoptosis. On the basis of these findings, PB1-F2 is proposed to kill host immune cells responding to influenza virus infection, either internally via virus infection, or externally in certain situations when the protein is released from infected cells under some circumstances. The proapoptotic properties of PB1-F2 expressed by IAV-infected cells may be related to its mitochondrial localization, since targeting green fluorescent protein to mitochondria through a PB1-F2 sequence, predicted to form an amphipathic alpha-helix, induces apoptosis in cells expressing the chimeric protein (17). We have proposed that proapoptotic proteins, together with lipids, form an apoptotic pore through which macromolecules

such as cytochrome *c* pass to activate caspase cascades (3–6, 27). Thus, we can determine whether PB1-F2 acts like other proapoptotic proteins by studying its interaction with planar phospholipid bilayer membranes.

A number of amphiphilic peptides and proteins are known to form ion conductive channels in membranes. Ionic channels have a number of characteristic features related to the fact that the aqueous pathway inside them is surrounded by a fixed set of amino acids. In general, ionic channels are marked by well-defined selectivity, voltage dependence, and distinct open channel conductance (24). Alternatively, polypeptides can promote the local breakdown of the membrane bilayer structure, creating a pore whose surface is formed completely or partially by polar lipid (7, 8, 15, 16, 27). Generally, the characteristics of these pores are not as well defined as those of ionic channels and are more dependent on membrane composition. Thus, both the character of the permeability changes and the degree of these changes for different cell lines may be quite different for channel-forming peptides and peptides that promote lipidic pore formation.

To further characterize the function of PB1-F2, we used a number of biophysical and electrophysiological techniques. Addition of tens of nanomoles of synthetic PB1-F2 (sPB1-F2) to planar phospholipid bilayer membranes caused an increase in the conductance of planar lipid bilayers and decreased their lifetime. Our data suggest that sPB1-F2 permeabilizes mem-

* Corresponding author. Mailing address: Laboratory of Cellular and Molecular Biophysics, National Institute of Child Health and Human Development, National Institutes of Health, Building 10, Room 10D14, Bethesda, MD 20892-1855. Phone: (301) 496-6571. Fax: (301) 402-0263. E-mail: joshz@helix.nih.gov.

branes in a manner different from typical ionic channel but consistent with lipidic or proteolipidic pore formation.

MATERIALS AND METHODS

Phospholipid membrane formation, current measurements, and chemicals. Two methods for planar phospholipid membrane formation were used in the present study. To study membrane conductance, we use relatively small areas of bilayers formed by the Montal-Mueller technique (20) with a 10-mg/ml lipid solution of diphytanoyl-*sn*-glycerophosphocholine (DPhC) or phosphatidylserine (PS) or mixtures of dioleoylphosphatidylcholine (DOPC)-dioleoylphosphatidylethanolamine (DOPE) (50%/50% [wt/wt]) or DOPC-DOPE-dioleoylphosphatidylserine (DOPS) (25%/25%/50% [wt/wt/wt]). The chamber, milled from Teflon, was similar to one described earlier (11a). It has two symmetrical compartments separated by a Teflon partition, and there are glass windows on both sides. For conductance measurements, the hole in the 0.025-mm-thick Teflon partition was 0.2 mm in diameter. A custom-made video microscope with a magnification of ×200 was used for visual control of membrane formation and quality. Both compartments were filled with 2.5-ml volumes of membrane bathing solution. Except where specifically indicated, all solutions were buffered with 10 mM HEPES at pH 7.5. To measure specific capacitance, surface tension, and membrane lifetime under different voltages, a large number of membranes must be studied, since dispersions are great (1). For these measurements, Mueller-Rudin-type planar phospholipid membranes (21) were used, as these were easier to form. Lipid bilayers were formed by applying a small amount of a lipid solution (10 mg/ml in hexadecane) onto a 0.3-mm-diameter hole in a Teflon film separating two buffer-filled compartments. The area of the bilayers was estimated with an accuracy of about 5%.

Ag/AgCl electrodes (In Vivo Metric, Ukiah, Calif.) were connected with the membrane bathing solution through 200-μl pipette tips with long thin ends filled with 2% agarose in 0.2 M KCl. An electrode placed in the *cis* compartment was connected to ground (zero potential). sPB1-F2 was added to the *cis* compartment (or in some experiments to both compartments), and the solution was stirred for 30 to 60 s using a miniature magnetic stirrer. The other electrode, in the *trans* compartment, was connected to the input of an Axopatch 200B voltage-clamp amplifier (Axon Instruments, Union City, Calif.).

Several experiments intended for low-noise signal recording were performed using the membrane patch technique. In this case, after the membrane was formed by the Montal-Mueller method, a glass pipette (with a tip 4 to 6 μm in diameter and with an Ag/AgCl electrode inside), mounted on a regular patch clamp holder, was placed in contact with the membrane. A second Ag/AgCl electrode was placed in the compartment opposite that containing the pipette, and patch formation was controlled by the standard technique of monitoring the system response to 5 mV, 60 Hz rectangular pulse. A fragment of membrane becomes tightly attached to the pipette tip and remains there after the pipette was moved off the membrane. The original membrane was then broken, and the membrane on the tip was used in the experiment.

Lipids, DPhC, DOPC, DOPE, and DOPS were purchased from Avanti Polar Lipids, Inc. (Alabaster, Ala.). Heptane, hexadecane, and salts were purchased from Sigma Chemical Corp. (St. Louis, Mo.). Solutions were prepared using deionized, double-distilled water. sPB1-F2 was synthesized with an ABI 433A automated peptide synthesizer on a 0.1 mM scale with 250 mg of TentaGel R-Trt-Ser(tertiary butyl) 9-fluorenylmethoxy carbonyl (Fmoc) resin (capacity 0.19 mmol/g) using the Fmoc/tertiary butyl strategy. The details of side chain protection, coupling steps, deprotection, and purification of sPB1-F2, as well as the characterization of the purified product by peptide sequencing, peptide mapping, and mass spectrometry will be described elsewhere (P. Henklein, unpublished data). A 0.25- or 0.5-mg/ml stock solution of the peptide in 0.1 M KCl was stored frozen in Eppendorf tubes at −70°C. After the stock solution was thawed, a portion of the peptide used for experiments was stored on ice for 1 to 2 days. (sPB1-F2 is very soluble in water even at the millimolar concentrations necessary for nuclear magnetic resonance structural studies, and it appears to be stable for long periods of time at room temperature as determined by nuclear magnetic resonance.) All experiments were performed at a controlled temperature of 26 to 29°C. Data were recorded on a computer disk using Axon Instruments Digidata 1322 A/D converter and pCLAMP 8.1 software.

Membrane surface tension and pore line tension. Membrane capacitance was determined from the capacitive current in response to the application of 25 V/s linear voltage sweeps with an amplitude of 25 mV. Surface tension was found by measuring the change in membrane capacitance under the given hydrostatic pressure gradient (26). Bilayer lifetimes were defined as the time from a step in voltage to the onset of irreversible membrane rupture.

Irreversible breakdown of bilayers in an electric field results from the devel-

opment of lipidic pores of an overcritical radius, which tend to spontaneous expansion (1, 15). The experimental dependencies of the mean membrane lifetime (averaged over no less than 10 measurements) on the voltage applied were fit with the theoretical expression based on this model described earlier (3, 14).

Preparation of large unilamellar vesicles (LUV). Lipid mixtures (typically, 1 μmol) were dried under a stream of nitrogen from CH_3Cl-methanol (2/1) solutions and further incubated under high vacuum for 2 to 3 h to remove residual traces of organic solvent. The dried lipids were dispersed in 1 ml of K^+ buffer (100 mM K_2SO_4, 10 mM HEPES, titrated with KOH to pH 7.0) by vortexing, freeze-thawed five times, and finally extruded 10 times through two stacked polycarbonate filters with a pore size of 0.1 μm. Vesicle lipid concentrations were quantified by phosphorous determination (2).

Assessment of increased LUV permeability by dissipation of transmembrane potential (Δψ). LUV prepared in K^+ buffer were diluted 100-fold in isosmotic Na^+ buffer (100 mM Na_2SO_4, 10 mM HEPES, titrated with NaOH to pH 7.0), and the dye $diSC_3$-(5) (3,3′-dipropylthiadicarbocyanine iodide) (Molecular Probes) was added from a 1 mM stock solution in Me_2SO_4 to a final concentration of 2 μM. After equilibration of the fluorescence signal for 5 to 10 min, valinomycin was added to create a negative-inside Δψ through selective efflux of vesicular K^+ ions, resulting in quenching of the dye's fluorescence. Permeation of solution ions across the liposome membrane was manifested by an increase in fluorescence of $diSC_3$-(5) due to loss of Δψ. Measurements were performed in an Amino-Bowman 8100 spectrofluorimeter, at 20°C, under constant stirring. The excitation and emission wavelengths were 645 and 670 nm, respectively (slit width, 4 nm). Values of $diSC_3$-(5) fluorescence recovery were estimated according to the equation $F_t = [(I_t − I_0)/(I_f − I_0)] × 100$, where F_t is fluorescence recovery at time t, I_t is fluorescence intensity observed at time t, I_0 is fluorescence intensity after the addition of valinomycin (final concentration, 1 nM), and I_f is fluorescence intensity after the addition of gramicidin (final concentration, 150 nM).

RESULTS

Conductance of lipid membrane treated with sPB1-F2. Addition of nanomolar concentrations of sPB1-F2 to the aqueous solution bathing DPhC membranes led to an increase of membrane conductance under almost every experimental condition tested. In a typical experiment, often with a −50 mV transmembrane potential on the side opposite to sPB1-F2 addition, conductance increased slowly and linearly, with an increase in membrane noise but without significant fluctuations. Occasionally, conductance increased abruptly 5 to 20 min after sPB1-F2 addition and then continued to increase slowly (Fig. 1A to C) but without the abrupt step-like fluctuations typical of ionic channels (Fig. 1F). At −80 to 100 mV, the fluctuations in the current induced by sPB1-F2 were significantly larger, but the membrane broke within 0.1 to 2 s after the onset of increased conductance. A similar pattern of conductance growth was observed even at the highest possible instrumental resolution and with smaller (low-noise) membranes attached to a micropipette tip (Fig. 1D and E). In an attempt to find conditions for channel-like sPB1-F2 insertion into membranes, we tested different membrane lipid compositions and membrane bathing solutions. However, we consistently observed a lack of abrupt step-like fluctuations despite different lipid and solution compositions: DPhC, PS, or membrane mixtures of DOPE-DOPC, DOPE-DOPC-cholesterol, or DOPE-DOPC-DOPS; a solution consisting of 0.15 M KCl, 1 mM $MgCl_2$, 1 mM EGTA, and 10 mM HEPES (pH 7.4); or individual monovalent or divalent cation solutions (0.1 M KCl, NaCl, 25 mM $CaCl_2$, $MgCl_2$) at pH 7.5 or 8.5.

When membranes either contained charged lipids or were bathed by divalent ion solutions, current noise induced by sPB1-F2 was significantly lower than for neutral membranes in monovalent cation solutions. Negatively charged membranes
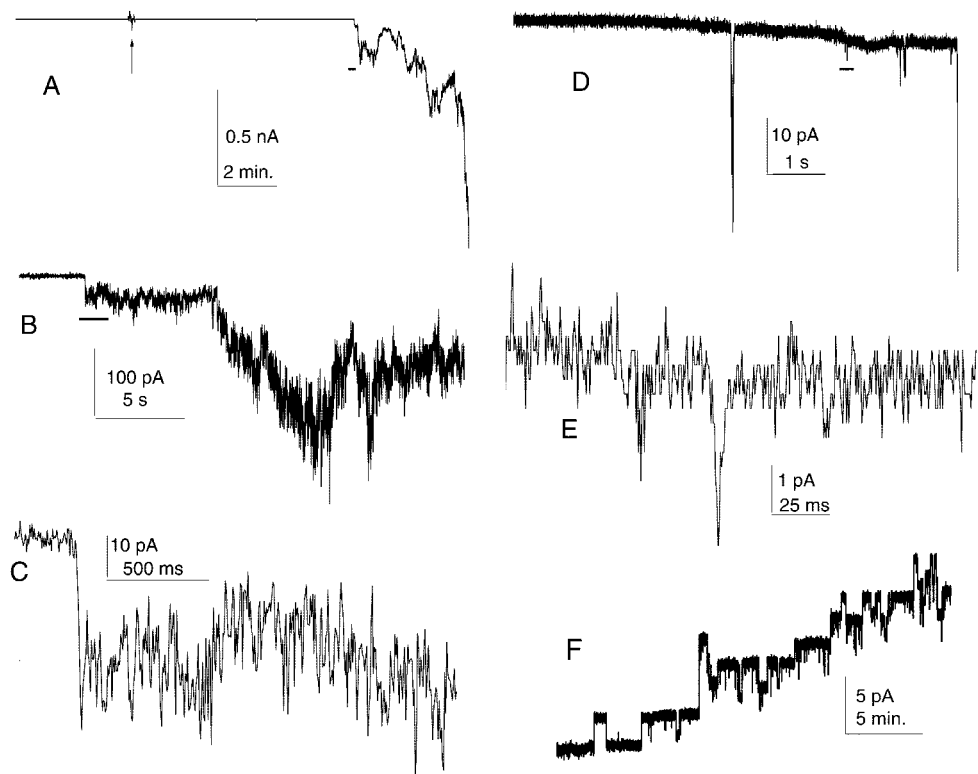
FIG. 1. Increase in conductance induced by sPB1-F2 in membrane. (A) Low-resolution record of the experiment. The arrow indicates the addition of 20 nM (final concentration) sPB1-F2 to the *cis* side of the membrane. (B to E) Medium-resolution (B and D) and high-resolution (C and E) records of sPB1-F2-induced fluctuations in conductance. Horizontal black bars in panels A, B, and D show the approximate position of the fragment expanded in the next panel. Discrete conductance levels visible in panel E are due to finite digitizer resolution. Recordings shown in panels A to C are obtained on a 0.2-mm-diameter membrane formed from DPhC in a solution consisting of 150 mM KCl, 1 mM MgCl$_2$, 1 mM EGTA, 1 mM dithiothreitol, and 20 mM HEPES (pH 7.4). Recordings shown in panels D and E are from DOPE-DOPC membrane on a 5-μm-diameter glass micropipette tip with 100 mM KCl–10 mM HEPES (pH 7.5) inside and outside the pipette. The membrane potential in both cases was −50 mV. (F) Membrane permeabilization by *S. aureus* alpha-toxin. The final concentration of *S. aureus* alpha-toxin was 30 nM. The membrane potential was +50 mV. The DOPC-DOPE membrane was formed in 0.1 M KCl–5 mM HEPES (pH 7.5). For all experiments, protein was added to the grounded compartments.

also required significantly higher concentrations of sPB1-F2 to register changes in conductance. At high salt concentration (1 M NaCl [pH 7.5]) and at acidic pH (DOPE-DOPC, 0.1 M NaCl [pH 6.0]), no conductance changes were observed prior to membrane breakdown with the addition of sPB1-F2 (0.2 to 1.5 μg/ml).

sPB1-F2 incorporation into membranes was strongly potential dependent. Negative potential on the side opposite to sPB1-F2 addition was favorable for the increase of membrane conductance, while positive potential almost inhibited conductance growth in PS-containing membranes and even reversed it in neutral membranes (Fig. 2).

Lipid membrane stability and line tension. A significant decrease in the stability of all types of membranes after the addition of peptide was noted during the conductance measurements described above. To quantify this effect, we measured the dependence of mean membrane lifetime on applied voltage for neutral and charged planar bilayer membranes in the presence and absence of 10 nM sPB1-F2 in both compartments of the membrane cell. In the range of voltages studied, peptide significantly decreased the mean membrane lifetime (Fig. 3). We also measured the specific capacitance and surface

tension of membranes made from mixtures of DOPC-DOPE (50%/50% [wt/wt]) or DOPC-DOPE-DOPS (25%/25%/50% [wt/wt/wt]), variables needed to estimate the line tension of the pores (Table 1). The least-squares fit of theoretical calculations to experimental data describes the dependence of the membrane lifetime on voltage well, leading to the calculation of pore line tension that decreases 1.4 or 1.8 times, compared to control, for charged or neutral membranes, respectively.

TABLE 1. Membrane-specific capacitance, membrane surface tension, and pore line tension[a]

Membrane composition or expt	Protein	Capacitance (μF/cm^2)	Surface tension (mN/m)	Line tension (10^{12})
DOPC-DOPE	PB1-F2	0.61 ± 0.01	0.79 ± 0.11	6.6
(50%/50%)	None	0.61 ± 0.01	1.04 ± 0.3	11.6
DOPC-DOPE-DOPS	PB1-F2	0.66 ± 0.01	0.29 ± 0.03	8.7
(25%/25%/50%)	None	0.67 ± 0.01	0.44 ± 0.07	12.1

[a] Experimental data are shown as means ± standard errors for 10 to 15 experiments. There was no sPB1-F2 added in control experiments.
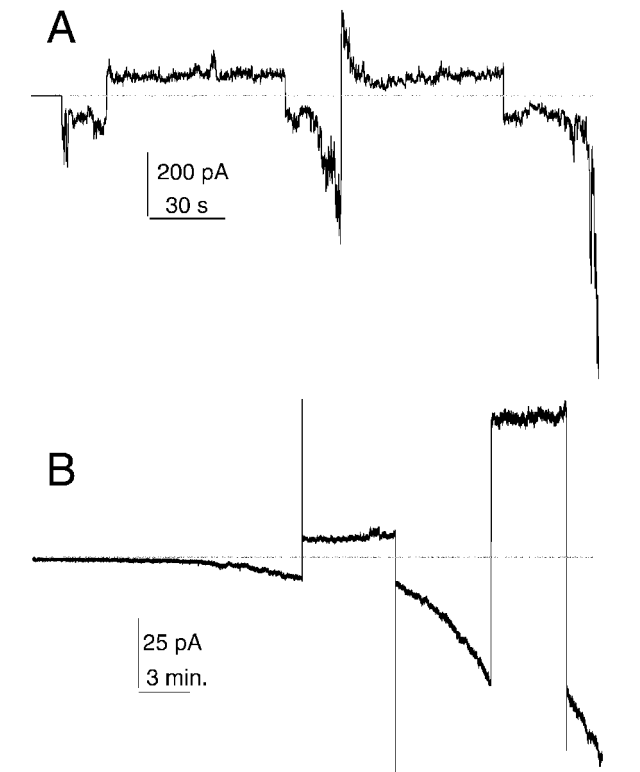
FIG. 2. Potential dependence of sPB1-F2 insertion into membrane. (A) sPB1-F2 (10 nM) was added to the *cis* (ground) side of the membrane approximately 5 min before the beginning of conductance increase. The membrane was formed from DPhC. (While it was not possible to obtain long records with DOPC-DOPE [50%/50%, wt/wt] membrane due to lower stability, qualitatively, the results were similar.) (B) sPB1-F2 (80 nM) was added approximately 15 and 30 min before the beginning of the record. The membrane was formed from DOPC-DOPE-DOPS (25%/25%/50% [wt/wt/wt]). In both cases, the membrane bathing solution contains 100 mM KCl–10 mM HEPES (pH 7.4). The horizontal line indicates zero current. The membrane potential was switched several times (first, −50 and second, +50 mV) and kept constant during positive or negative fragments of current traces.
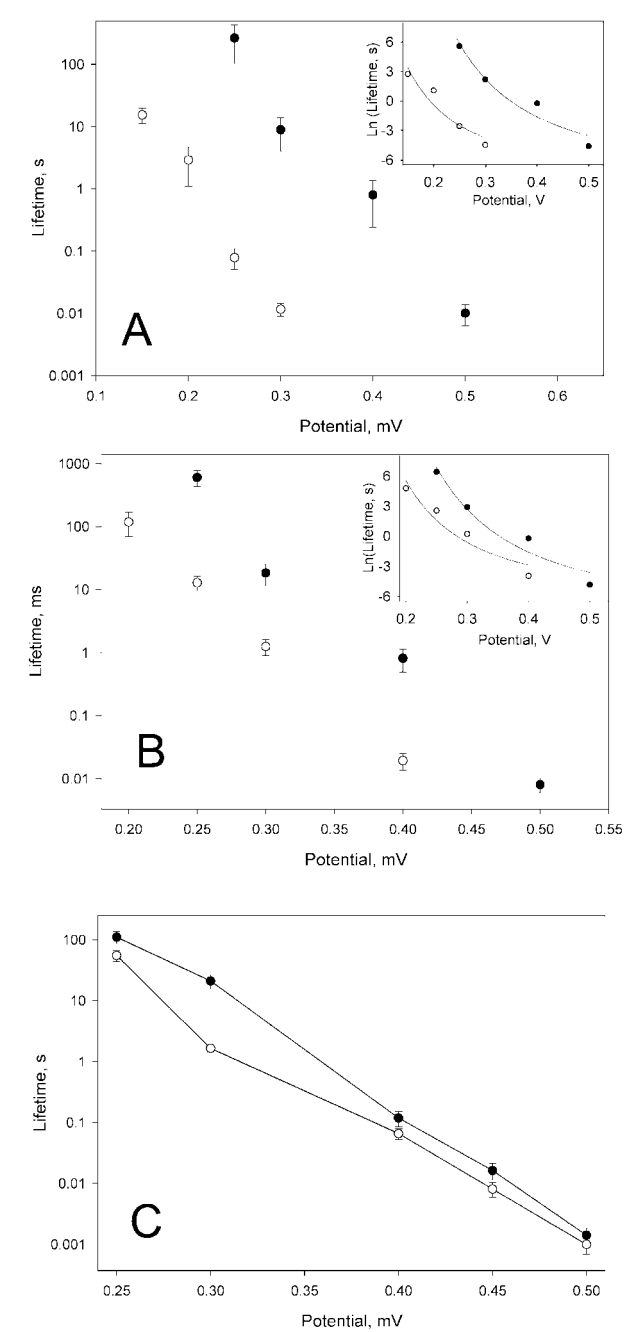

FIG. 3. Potential dependence of protein-induced decrease in membrane lifetime. (A) Effect of sPB1-F2 on membrane formed from neutral lipid mixture DOPE-DOPC (50%/50% [wt/wt]). (B) Effect of sPB1-F2 on membrane formed from the mixture that contains charged lipid DOPE-DOPC-DOPS (25%/25%/50% [wt/wt/wt]). (C) Effect of *S. aureus* alpha-toxin on membrane formed from egg phosphatidylcholine-cholesterol (3/1). The mean values ± standard errors (error bars) from 10 to 15 experiments are plotted in conventional form. The inserts show the same data and theoretical fit, plotted as Ln(lifetime) versus voltage in order to balance curve-fitting error over the wide range of experimental values. Control experiments (●) and experiments performed with 10 nM sPB1-F2 (○) (A and B) or 12 nM alpha-toxin (C) on both sides of membrane are shown. The membrane bathing solution in panels A and B was 0.1 M KCl–10 mM HEPES (pH 7.4); the membrane bathing solution in panel C was 0.1 M KCl–1 mM EDTA–10 mM Tris citrate (pH 7.5).
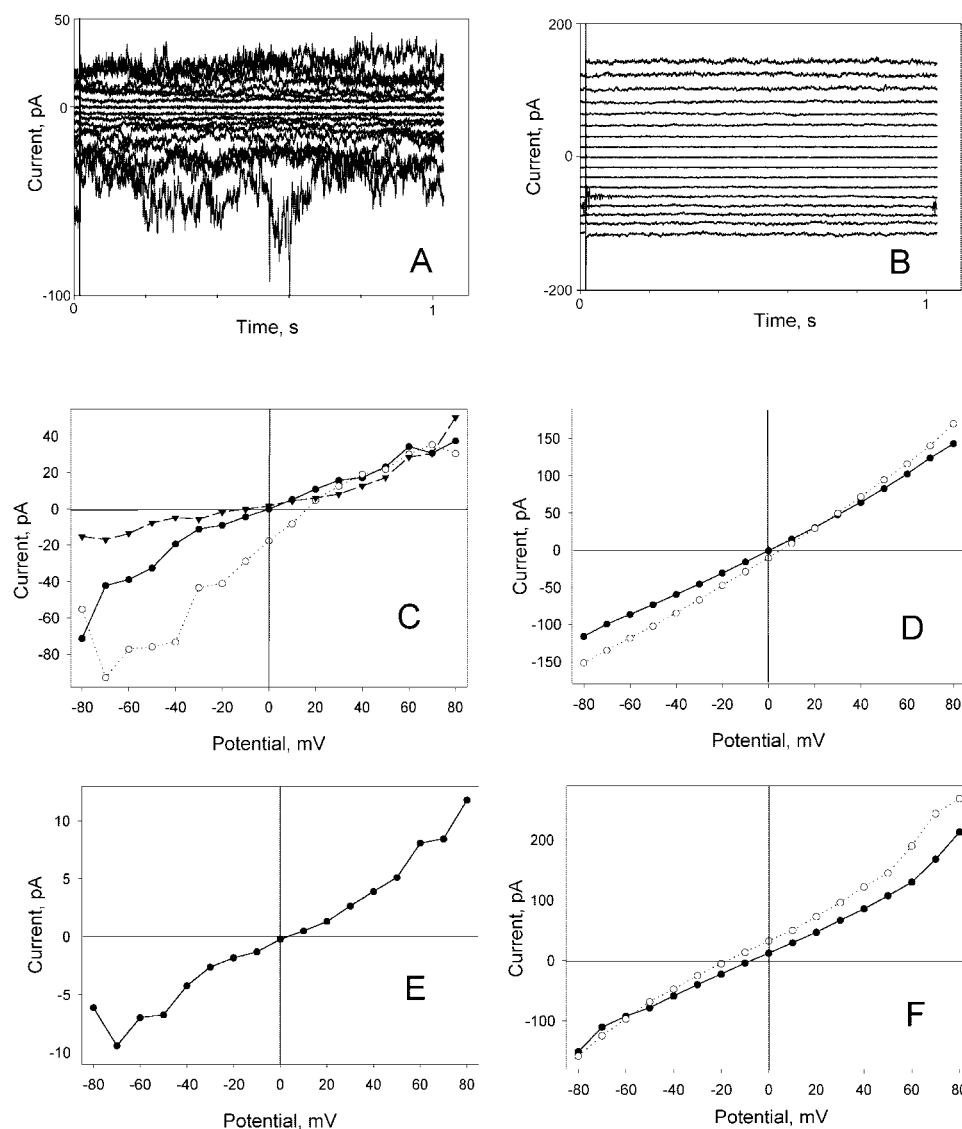
TABLE 2. Effects of different proteins, peptides, and lysophosphocholine on membrane lifetime and pore line tension

Effector	Line tension (γ, pN)	$\gamma_{control}/\gamma$	Lifetime decrease[a]
PB1-F2 (10 nM)[b]	6.6, 8.7	1.8, 1.4	10^3, 10^2
tBcl-x_L (15 nM)[c]	4	2	10^2
Bax (0.1–0.15 nM)[d]	7.7	1.2	10
gp41 (2 μM)[e]	6.6	1.5	10^2
c-Bid (15 nM)[f]	2.9	1.3	25
Lyso-PC (300 nM)[g]	ND[h]	ND	10
Alpha-toxin	ND	ND	2

[a] $\gamma_{control}/\gamma$ averaged for several voltages, either calculated or estimated from figures in the papers cited.
[b] The first value shows the value for neutral membrane, and the second value shows the value for charged membrane.
[c] Data from Basañez et al. (5).
[d] Data from Basañez et al. (3).
[e] Data from Chernomordik et al. (14).
[f] Data from G. Basañez (personal communication).
[g] Lyso-PC, lysophosphocholine. Data from Basañez et al. (4).
[h] ND, no data.

FIG. 4. Current voltage characteristics of sPB1-F2-modified membranes. (A and B) Current traces of sPB1-F2-treated membrane at −80 to +80 mV potentials (*cis* ground) with 10 mV increment. The membrane was DPhC membrane bathed in symmetrical 0.1 M NaCl solution (A) or DOPE-DOPC-DOPS (25%/25%/50% [wt/wt/wt]) membrane bathed in symmetrical 0.1 M KCl solution (B). (C) Dependence of electric current (I) and electrical potential (V) of sPB1-F2-treated DPhC membrane in symmetrical 0.1 M NaCl (●), 0.1 M NaCl in the *trans* compartment and 0.35 M NaCl in the *cis* compartment (○), and after the addition of 5 mM $CdCl_2$ to the *cis* compartment ▼. (D) Dependence of I and V of sPB1-F2-treated DOPE-DOPC-DOPS (25%/25%/50% [wt/wt/wt]) membrane in symmetrical 0.1 M KCl (●) and 0.1 M KCl in the *trans* compartment and 0.25 M KCl in the *cis* compartment (○). (E) Dependence of I and V on sPB1-F2-treated DPhC membrane in 0.1 M NaCl in the *cis* compartment and 0.1 M KCl in the *trans* compartment. (F) Dependence of I and V of sPB1-F2-treated DPhC membrane formed in asymmetrical solutions, 5 mM $MgCl_2$ in the *cis* compartment and 25 mM $MgCl_2$ in the *trans* compartment (○) and after the addition of 5 mM $CdCl_2$ to the *cis* compartment (●).

In order to compare the membrane-destabilizing activity of sPB1-F2 to that of some known channel-forming protein, we tested *S. aureus* alpha-toxin (molecular mass of 34 kDa). Two-sided addition of alpha-toxin, at roughly the same molar concentration as that of sPB1-F2, had a much smaller destabilizing effect on planar membranes compared not only to sPB1-F2 but also to other known membrane-destabilizing agents (Fig. 3 and Table 2).

Divalent and monovalent cation permeability. As discussed above, addition of sPB1-F2 always resulted in a significant decrease in membrane stability. The membrane usually broke soon after the onset of increased conductance, at a relatively low conductance level (under 10 nS). Due to this membrane instability in the presence of sPB1-F2, it was not possible to study membrane selectivity by using approaches that require perfusion of the chamber to wash out unbound protein and at least one more perfusion to change ionic composition of the bathing solution. However, it was sometimes possible to change the ionic composition of the bathing solution by adding small volumes of concentrated salt to the *cis* or *trans* compart-

TABLE 3. Ion selectivity of planar phospholipid bilayer membranes modified by sPB1-F2

Bathing solutions and membrane composition[a]	Reversal potential (mV)[b]	Selectivity
NaCl/NaCl (0.1 M/0.35 M) *PC/PE/PS (50%/30%/20%)*	14 ± 3.6	$P_{Na}/P_{Cl} = 2.9$
KCl/KCl (0.1 M/0.25 M) *PC/PE/PS (50%/30%/20%)*	6.5 ± 0.5^{c}	$P_{K}/P_{Cl} = 1.8$
KCl/KCl (0.1 M/0.25 M) *DPhC*	9 ± 1^{c}	$P_{K}/P_{Cl} = 2.4$
KCl/NaCl (0.1 M/0.1 M) *DPhC*	0 ± 3^{c}	$P_{K}/P_{Na} = 1$
MgCl$_2$/MgCl$_2$ (5 mM/25 mM) *DPhC*	-24 ± 3.9	$P_{Mg}/P_{Cl} = 0.15$

[a] Compositions and concentrations of the electrolytes separated by the membrane are given as *trans/cis*. Membrane composition is shown in italic type. PC, phosphocholine; PE, phosphatidylethanolamine; PS, phosphatidylserine.

[b] A concentration or composition gradient of electrolytes was formed across a lipid bilayer in presence of 10 to 40 nM sPB1-F2. Under these conditions, ions diffuse across the bilayer according to the ion selectivity of pores. Gradients of permeant ions will create potentials. These potentials were determined here by measuring the current reversal potential, i.e., the external potential that had to be applied in order to make the current through the lipid bilayer zero. Reversal potentials were used to calculate the relative pore selectivity, defined as the ratios of the pore permeability for different ions. Unless indicated otherwise, data are mean $\pm$ standard deviation for three or four measurements.

[c] Average of two measurements $\pm$ maximum deviation.

ment with stirring. In order to minimize error due to incorporation of additional sPB1-F2 molecules into the membrane, it was held at +50 mV potential during these manipulations.

In symmetric solutions, current/voltage characteristics of membranes modified by sPB1-F2 were linear at low membrane potentials (Fig. 4). However, some deviations from linearity were often observed at potentials above 30 to 40 mV, especially for noncharged membranes. These deviations were most likely caused by large fluctuations of membrane permeability (e.g., Fig. 4A). Both negatively charged (PS) and neutral membranes showed cationic over anionic selectivity but no preference between potassium and sodium ions (Fig. 4C to E and Table 3). Addition of 5 mM CdCl$_2$ to the *cis* compartment reduced current at negative potentials by 70 to 80% in NaCl solutions and by 40 to 50% in KCl solutions. Neither CaCl$_2$ nor MgCl$_2$ reduced sPB1-F2-induced conductance, but at 60 mM, either CaCl$_2$ or MgCl$_2$ added asymmetrically (added to only one of the two compartments) to a 100 mM NaCl bathing solution did cause an anionic shift of current reversal potential (data not shown).

Direct measurements of relative permeability of Mg or Cl ions were performed on DPhC membranes in asymmetrical MgCl$_2$ solutions (solution in one compartment) (5 and 25 mM). The reversal potential of -24 mV obtained with a MgCl$_2$ gradient demonstrated that while both magnesium and chloride ions permeate the pores induced by sPB1-F2, chloride permeability is significantly higher. In addition, Cd^{2+} ions did not block transmembrane current in MgCl$_2$ solution (Fig. 4F).

Effect of sPB1-F2 on liposome permeability. We have previously shown that Bax-like proapoptotic proteins not only decrease bilayer lipid membrane stability and line tension but also efficiently induce the release of different markers en-
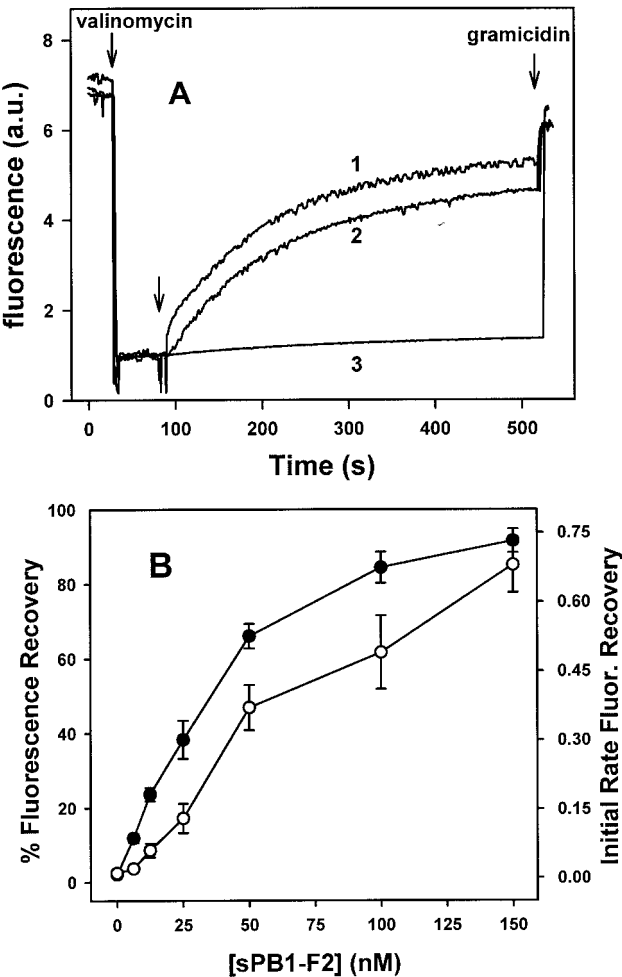

FIG. 5. Loss of transmembrane potential induced by PB1-F2 in LUV. (A) DOPC-cholesterol (3/1) LUV with fluorescent dye diSC$_3$-(5) were prepared as described in Materials and Methods. The addition of valinomycin (first arrow) created a negative-inside transmembrane potential ($\Delta\psi$), which led to quenching of the dye's fluorescence. At the time indicated by the second arrow, 50 nM *S. aureus* alpha-toxin (curve 1), 50 nM sPB1-F2 (curve 2), or buffer alone (curve 3) was added, and $\Delta\psi$ loss was monitored by recovery of the fluorescence signal. Finally, gramicidin was added (third arrow) to completely dissipate the LUV transmembrane potential. The similarity in the time courses of potential dissipation by PB1-F2 and alpha-toxin indicates that it is more likely that sPB1-F2 forms pores than ruptures membrane. Fluorescence is given in arbitrary units (a.u.). (B) Dissipation of vesicular $\Delta\psi$ as a function of sPB1-F2 concentration. DOPC LUV were treated with different amounts of sPB1-F2, and the values of the maximal extent (●) and initial rate (○) of diSC$_3$-(5) fluorescence (Fluor.) recovery were estimated as explained in Materials and Methods. Data are averages $\pm$ standard errors (error bars) of triplicate determinations of at least two independent LUV populations. Other conditions are as explained above for panel A. Note that the extravesicular compartment is equivalent to *cis* or the ground side of the planar membrane.

trapped within pure lipid vesicles (4). However, addition of sPB1-F2 to the suspension of liposomes without any experimentally imposed transmembrane potential had no significant effect on membrane permeability. Even at protein/lipid ratios as high as 1:50, sPB1-F2 induced only a small extent of ANTS/

DPX (8-aminonaphthalene-1,3,6-trisulfonic acid/*p*-xylene-bis-pyridinium bromide) release from vesicles (around 5 to 10% in DOPC LUV and less than 5% in DOPC-DOPS [50%/50%] LUV [data not shown]). In contrast, addition of either sPB1-F2 or *S. aureus* alpha-toxin to DOPC-cholesterol (3/1) lipid vesicles with a potential gradient across the membrane rapidly initiated ion leakage and membrane potential dissipation (Fig. 5A). A similar dose-dependent effect of sPB1-F2 was observed on pure DOPC (Fig. 5B) or DOPC-DOPS vesicles (not shown), while the effect of *S. aureus* alpha-toxin on DOPC LUV was minimal under these conditions (in agreement with the known requirement for cholesterol of this toxin to form channels). sPB1-F2 affected neither the fluorescence of diSC$_3$-(5) in LUV prepared with internal and external Na$^+$ buffer and treated with valinomycin nor the scattering of LUV suspension, demonstrating that sPB1-F2 did not cause $\Delta\Psi$ loss through major rearrangements in vesicle structure such as fragmentation or "leaky" fusion (data not shown).

DISCUSSION

Since sPB1-F2 induces apoptosis in cells to which it is added, its mechanism of action on purely lipid membranes was studied here. sPB1-F2 caused profound membrane permeability changes in planar bilayers. These changes in permeability were variable in amplitude and weakly selective. Taking advantage of the large surface tension of planar phospholipid bilayer membranes, we could estimate the tendency of PB1-F2 to stabilize the edges of bent pores by measuring the membrane lifetime as a function of transmembrane voltage. These results were consistent with the hypothesis that PB1-F2 forms pores in lipid membranes that are at least partially lipidic. Such poration activity could explain the ability of PB1-F2 to cause apoptosis naturally, when it is expressed in infected cells. It is not known yet whether PB1-F2 is released from infected cells, but if so, it could enter bystander cells by sliding along the edge of its own lipidic pore in the plasma membrane of the bystander cell and then diffuse to the mitochondria to open an apoptotic pore. Apoptogenic macromolecules, such as cytochrome *c*, would then escape into the cytosol to activate a cascade of caspases that execute apoptosis.

sPB1-F2 is another instance of a proapoptotic protein that permeabilizes and destabilizes planar lipid membranes such as Bax, cleaved Bcl-xl, and P828-the amphiphilic helix of HIV gp41 (3, 5, 14). Pore formation by these proteins is associated with a significant degree of membrane destabilization indicating lipidic pore formation rather than insertion and opening of a purely proteinaceous channel. Another viral cell killing protein, HIV-1 Vpr has been shown to form cation-selective ion channels in planar lipid bilayers and can cause an inward sodium current in living cells (22, 23). While Vpr was not tested for the membrane destabilizing effect, Vpr induced conductance changes (23) are more consistent with lipidic pores (6) than with proteinaceous channels. Typical protein channel formers (alamethicin and α-latrotoxin [10, 16a]) have distinctive abrupt step-like fluctuations in conductance and usually have high ion selectivity. Cytolytic peptides (mellitin, magainins, and cecropins [18, 19, 25]) usually have moderate ion selectivity and produce a wide range of conductance fluctua-

tions in the membrane: an indication of the proteolipidic nature of pores formed.

Membrane permeabilization by sPB1-F2 is different from both ion channel and cytolytic proteins. In sPB1-F2-treated membranes at 50 mV, except for the first abrupt conductance increase in rare cases, we fail to observe distinctive conductance levels or large transient conductance fluctuations with any of the experimental conditions employed using the highest-resolution instrument (Fig. 1). sPB1-F2 has low ion selectivity, with predominantly cationic selectivity in KCl or NaCl solutions and predominantly anionic in Mg^{2+} or Ca^{2+} chloride solutions (Fig. 4 and Table 3). Interestingly, sPB1-F2 has specific sensitivity to Cd^{2+} ions, a feature of some cellular ion channels, not known for exogenous cytolytic proteins.

The sPB1-F2 amino acid sequence predicts a net positive charge for this molecule (5 negative and 15 positive residues, theoretical pI of 10.75) at neutral pH. This provides a facile explanation for the potential dependence of PB1-F2 membrane incorporation. Negative potential on the side opposite that of sPB1-F2 addition creates an intramembrane field gradient favorable for the movement of positively charged molecules from the surface into the hydrophobic region of the phospholipid bilayer (10). A correspondingly positive potential in the *trans* compartment must have the opposite effect. This is exactly what we observed in experiments with planar bilayers and liposomes with negatively charged inner volume. Taking into account the high positive potential on the outer surface of inner mitochondrial membrane, this may explain why PB1-F2 accumulates predominantly on this membrane (17) where it could do the most damage to mitochondrial homeostasis. Passing through the mitochondrial outer membrane may involve one of the mitochondrion's known protein transport mechanisms including porin channels that are big enough for passage of comparably sized molecules. The significantly higher sPB1-F2 concentration required to permeabilize PS-containing membranes compared to membranes formed exclusively from zwitterionic lipids is most likely caused by strong binding and partial neutralization of the positive charges of the protein by negatively charged PS head groups.

What is the mechanism of PB1-F2-induced membrane permeabilization and how can it be related to its putative cytotoxicity? Like other proapoptotic proteins, PB1-F2 dramatically decreases mean membrane lifetime in an electric field (Fig. 3 and Table 2). This can be interpreted as the promotion of lipidic pore formation due to a decrease in pore line tension (1, 15). Indeed, the line tension values calculated from our present data (Table 1) are significantly lower for membranes in the presence of sPB1-F2 compared to control. Quantitatively, line tension in the presence of 10 nM sPB1-F2 decreases 1.4- to 1.8-fold, while mean lifetime decreases by 2 to 3 orders of magnitude. These numbers are close to those reported for Bax, cleaved Bcl-x$_L$, and human immunodeficiency virus gp41 (3, 5, 14; also summarized in Table 2) (A common misinterpretation of these kinds of experiments is the assumption that protein capable of breaking a planar membrane is capable of breaking the cell membrane. Actually, the similarity of in vitro and in vivo actions of the protein is more likely limited to its ability to promote initial pore formation. In planar membrane, which is always under tension, this leads to membrane breakage, while

in the unstressed cellular membrane, pore formation may be the end of the physical part of the process).

How are we to imagine relatively large protein molecules changing the overall lipid organization resulting in diminished line tension? The theory of membrane destabilization via a decrease in pore line tension was developed for small detergent molecules or lipids that mix with membrane lipids in high ratios and alter the intrinsic curvature of the membrane monolayer (13). More recently, it was suggested that magainin 2 and other antimicrobial peptides permeabilize membranes in a detergent-like manner, i.e., by induction of curvature changes upon insertion (16b, 25). However, magainin, mellitin, and similar peptides form pores in planar membranes at much higher concentrations than do the proapoptotic proteins. They are also significantly smaller (under 3 kDa) than Bax (21 kDa [3]), cleaved Bcl-x_L (15 kDa [5]), or sPB1-F2 (10.5 kDa). The sizes of the latter polypeptides are closer to the sizes of typical exogenous channel-forming proteins (e.g., alpha-toxin from *Staphylococcus aureus* [34 kDa] and sea anemone toxins [15 to 20 kDa] [9, 11]) than to detergent-like membrane active agents (e.g., lysolecithin [564 Da]). Accordingly, the mechanism of their action may also be different from a simple, curvature-related action of small molecules, although an asymmetry in the packing volumes of a protein in its head group region compared to the effective volume of the protein that resides in the tail group region would certainly generate the positive monolayer curvature that forms lipidic pores. It seems possible that incorporation of a large amphiphilic molecule into a membrane initially forms a small, half lipid and a half protein pore that can later increase in size if the protein is capable of forming multimolecular aggregates in the lipid bilayer. Since we did not detect long-living large pores during incorporation of sPB1-F2 into the membrane at low potentials, it is unlikely that this protein forms stable multimolecular aggregates in the plane of the membrane instantly (Fig. 1). However, the large current fluctuations that were observed at high potentials (Fig. 4A) indicate that large pores, with lifetimes in the millisecond range, may form later in a potential-dependent manner. In addition to a certain degree of initial permeabilization of the membrane, the hydrophilic/hydrophobic mismatch in lipid bilayer packing around the protein is likely to reduce the energy cost of the following pore enlargement that is equivalent to a decrease in the pore line tension measured experimentally. Thus, sPB1-F2 is similar to Bax, cleaved Bcl-xl, and human immunodeficiency virus gp41 that probably form aggregates in the bilayer that stabilize larger proteolipidic pores (3, 5, 14). In contrast, a typical channel-forming protein, *S. aureus* alpha-toxin at roughly the same concentration, causes much lower membrane destabilization than sPB1-F2 (Fig. 3 and Table 2). This indicates that membrane destabilization is not a simple result of any protein incorporation into bilayer but a specific feature of a particular protein structure.

In summary, this novel proapoptotic IAV protein forms potential-dependent lipidic pores in planar phospholipid bilayers that initiate the breakdown of bilayer structure. When this effect is quantified as line tension, we see that the ability of this protein to permeabilize and disrupt purely lipidic membranes is the same as other proapoptotic proteins, indicating that viral proapoptotic proteins may form pores in the mitochondrial membrane with no or minimal participation (after initial spe-

cific binding) of cellular proteins. The interaction of the positively charged amphipathic helix of PB1-F2 with lipid head group charges and transmembrane electric field plays an important role in its incorporation into the membrane and resulting pore formation. To kill cells effectively, it may be sufficient if exogenous molecules form a nonspecific ion leakage passageway through small pores in the inner mitochondrial membrane or facilitate formation of large proteolipidic pores in the outer mitochondrial membrane (3, 5) under certain conditions (high transmembrane potential on the mitochondrial inner membrane or membrane lateral tension due to swelling, respectively). The similarity in action of different apoptotic proteins on artificial membranes may point to some common mechanism worthy of further investigation.

REFERENCES

1. **Abidor, I. G., V. B. Arakelyan, L. V. Chernomordik, Y. A. Chizmadzhev, V. F. Pastushenko, and M. R. Tarasevich.** 1979. Electrical breakdown of BLM: main experimental facts and their qualitative discussion. Bioelectrochem. Bioenerget. **6:**37–52.
2. **Barlett, G. R.** 1959. Phosphorus assay in column chromatography. J. Biol. Chem. **234:**466–468.
3. **Basañez, G., A. Nechushtan, O. Drozhinin, A. Chanturiya, E. Choe, S. Tutt, K. A. Wood, Y.-T. Hsu, J. Zimmerberg, and R. J. Youle.** 1999. Bax, but not Bcl-x_L, decreases the lifetime of planar phospholipid bilayer membranes at subnanomolar concentrations. Proc. Natl. Acad. Sci. USA **96:**5492–5497.
4. **Basañez, G., J. C. Sharpe, J. Galanis, T. B. Brandt, J. M. Hardwick, and J. Zimmerberg.** 2002. Bax-type apoptotic proteins porate pure lipid bilayers through a mechanism sensitive to intrinsic monolayer curvature. J. Biol. Chem. **277:**49360–49365.
5. **Basañez, G., J. Zhang, B. N. Chau, G. I. Maksaev, V. A. Frolov, T. A. Brandt, J. Burch, J. M. Hardwick, and J. Zimmerberg.** 2001. Pro-apoptotic cleavage products of Bcl-xL form cytochrome *c*-conducting pores in pure lipid membranes. J. Biol. Chem. **276:**31083–31091.
6. **Basañez, G., and J. Zimmerberg.** 2001. HIV and apoptosis: death and the mitochondrion. J. Exp. Med. **193:**F11–F14.
7. **Bashford, C. L., G. M. Alder, G. Menestrina, K. J. Micklem, J. J. Murphy, and C. A. Pasternak.** 1986. Membrane damage by hemolytic viruses, toxins, complement, and other cytotoxic agents. A common mechanism blocked by divalent cations. J. Biol. Chem. **261:**9300–9308.
8. **Benz, R., F. Beckers, and U. Zimmermann.** 1979. Reversible electrical breakdown of lipid bilayer membranes: a charge-pulse relaxation study. J. Membr. Biol. **48:**181–204.
9. **Bhakdi, S., H. Bayley, A. Valeva, I. Walev, B. Walker, M. Kehoe, and M. Palmer.** 1996. Staphylococcal alpha-toxin, streptolysin-O, and Escherichia coli hemolysin: prototypes of pore-forming bacterial cytolysins. Arch. Microbiol. **165:**73–79.
10. **Chanturiya, A. N., and V. K. Lishko.** 1992. Potential dependent α-latrotoxin interaction with black lipid membranes. Toxicon **30:**1059–1064.
11. **Chanturiya, A. N., O. Y. Shaturskji, V. K. Lishko, M. M. Monastyrnaya, and E. P. Kozlowskaya.** 1990. Interaction of a toxin from the sea anemone *Radianthus macrodactylus* with bilayer lipid membranes. Biol. Membr. **4:**1251–1262.
11a.**Chanturiya, A., M. Whitaker, and J. Zimmerberg.** 1999. Calcium-induced fusion of sea urchin egg secretory vesicles with planar phospholipid bilayer membranes. Mol. Membr. Biol. **16:**89–94.
12. **Chen, W., P. A. Calvo, D. Malide, J. Gibbs, U. Schubert, I. Bacik, S. Basta, R. O'Neill, J. Schickli, P. Palese, P. Henklein, J. R. Bennink, and J. W. Yewdell.** 2001. A novel influenza A virus mitochondrial protein that induces cell death. Nat. Med. **7:**1306–1312.
13. **Chernomordik, L., A. Chanturiya, J. Green, and J. Zimmerberg.** 1995. The

hemifusion intermediate and its conversion into complete fusion: regulation by membrane composition. Biophys. J. **69:**922–929.

14. **Chernomordik, L., A. N. Chanturiya, E. Suiss-Toby, E. Nora, and J. Zimmerberg.** 1994. An amphipathic peptide from the C-terminal region of the human immunodeficiency virus envelope glycoprotein causes pore formation in membranes. J. Virol. **68:**7115–7123.

15. **Chernomordik, L. V., and Y. A. Chizmadzhev.** 1989. Electroporation of bilayer lipid membranes: phenomenology and mechanism, p. 181–192. *In* E. Neumann, A. Sowers, and C. Jordan (ed.), Electroporation and electrofusion in cell biology. Plenum Press, New York, N.Y.

16. **Cruciani, R. A., J. L. Barker, S. R. Durell, G. Raghunathan, H. R. Guy, M. Zasloff, and E. F. Stanley.** 1992. Magainin 2, a natural antibiotic from frog skin, forms ion channels in lipid bilayer membranes. Eur. J. Pharmacol. **226:**287–296.

16a.**Duclohier, H., and H. Wroblewski.** 2001. Voltage-dependent pore formation and antimicrobial activity by alamethicin and analogues. J. Membr. Biol. **184:**1–12.

16b.**Epand, R. M.** 1998. Lipid polymorphism and protein-lipid interactions. Biochim. Biophys. Acta **1376:**353–368.

17. **Gibbs, J. S., D. Malide, F. Hornung, J. R. Bennink, and J. W. Yewdell.** 2003. The influenza A virus PB1-F2 protein targets the inner mitochondrial membrane via a predicted basic amphipathic helix that disrupts mitochondrial function. J. Virol. **77:**7214–7224.

18. **Ladokhin, A. S., and S. H. White.** 2001. ′Detergent-like′ permeabilization of anionic lipid vesicles by melittin. Biochim. Biophys. Acta **1514:**253–260.

19. **Matsuzaki, K., K. Sugishita, N. Ishibe, M. Ueha, S. Nakata, K. Miyajima, and R. M. Epand.** 1998. Relationship of membrane curvature to the formation of pores by magainin 2. Biochemistry **37:**11856–11863.

20. **Montall, M., and P. Mueller.** 1972. Formation of biomolecular membranes from lipid monolayers and a study of their electrical properties. Proc. Natl. Acad. Sci. USA **69:**3561–3566.

21. **Mueller, P., D. O. Rudin, T. Tien, and W. C. Westcott.** 1962. Reconstitution of cell membrane in vitro and its transformation into an excitable system. Nature **194:**979–980.

22. **Piller, S. C., G. D. Ewart, D. A. Jans, P. W. Gage, and G. B. Cox.** 1999. The amino-terminal region of Vpr from human immunodeficiency virus type 1 forms ion channels and kills neurons. J. Virol. **73:**4230–4238.

23. **Piller, S. C., G. D. Ewart, A. Premkumar, G. B. Cox, and P. W. Gage.** 1996. Vpr protein of human immunodeficiency virus type 1 forms cation-selective channels in planar lipid bilayers. Proc. Natl. Acad. Sci. USA **93:**111–115.

24. **Sansom, M. S. P.** 1991. The biophysics of peptide models of ion channels. Prog. Biophys. Mol. Biol. **55:**139–235.

25. **Shai, Y.** 1999. Mechanism of the binding, insertion and destabilization of phospholipid bilayer membranes by alpha-helical antimicrobial and cell non-selective membrane-lytic peptides. Biochim. Biophys. Acta **1462:**55–70.

26. **Sukharev, S. I., L. V. Chernomordik, I. G. Abidor, and Y. A. Chizmadzhev.** 1992. Effects of uranyl ions on the properties of bilayer lipid membranes. Bioelectrochem. Bioenerget. **9:**133–140.

27. **Zimmerberg, J.** 1999. Hole-istic medicine. Science **284:**1516–1519.